Article

Reaction of Molecular Oxygen with a Pd-Hydride To Produce a Pd-Hydroperoxide: Experimental Evidence for an HX-Reductive-Elimination Pathway

Michael M. Konnick, and Shannon S. Stahl

J. Am. Chem. Soc., **2008**, 130 (17), 5753-5762 • DOI: 10.1021/ja7112504 • Publication Date (Web): 05 April 2008

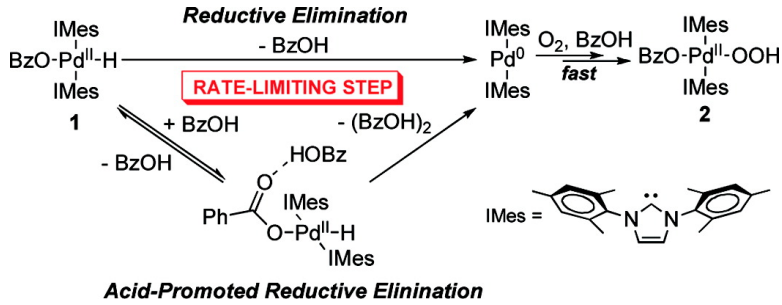

More About This Article

Additional resources and features associated with this article are available within the HTML version:

- Supporting Information
- Links to the 4 articles that cite this article, as of the time of this article download
- Access to high resolution figures
- Links to articles and content related to this article
- Copyright permission to reproduce figures and/or text from this article

View the Full Text HTML

J|A|C|S
ARTICLES

Published on Web 04/05/2008

Reaction of Molecular Oxygen with a Pd^{II}-Hydride To Produce a Pd^{II}-Hydroperoxide: Experimental Evidence for an HX-Reductive-Elimination Pathway

Michael M. Konnick and Shannon S. Stahl*

Department of Chemistry, University of Wisconsin−Madison, 1101 University Avenue, Madison, Wisconsin 53706

Received December 19, 2007; E-mail: stahl@chem.wisc.edu

Abstract: The reaction of molecular oxygen with a Pd^{II}-hydride species to form a Pd^{II}-hydroperoxide represents one of the proposed catalyst reoxidation pathways in Pd-catalyzed aerobic oxidation reactions, but well-defined examples of this reaction were discovered only recently. Here, we present a mechanistic study of the reaction of O_2 with *trans*-$(IMes)_2Pd(H)(OBz)$, **1** (IMes = 1,3-dimesitylimidazol-2-ylidene), which yields *trans*-$(IMes)_2Pd(OOH)(OBz)$, **2**. The reaction was monitored by ^1H NMR spectroscopy in benzene-d_6, and kinetic studies reveal a two-term rate law, rate $= k_1[\mathbf{1}] + k_2[\mathbf{1}][BzOH]$, and a small deuterium kinetic isotope effect, $k_{Pd-H}/k_{Pd-D} = 1.3(1)$. The rate is independent of the oxygen pressure. The data support a stepwise mechanism for the conversion of **1** into **2** consisting of rate-limiting reductive elimination of BzOH from **1** followed by rapid reaction of molecular oxygen with $(IMes)_2Pd^0$ and protonolysis of a Pd−O bond of the η^2-peroxo complex $(IMes)_2Pd(O_2)$. Benzoic acid and other protic additives (H_2O, ArOH) catalyze the oxygenation reaction, probably by stabilizing the transition state for reductive elimination of BzOH from **1**. This study provides the first experimental validation of the mechanism traditionally proposed for aerobic oxidation of Pd-hydride species.

Introduction

Palladium-catalyzed reactions are among the most versatile methods for the selective aerobic oxidation of organic molecules. These reactions have been proposed to proceed via a Pd^{II}/Pd^0 catalytic cycle in which Pd^{II} mediates substrate oxidation and Pd^0 is reoxidized by molecular oxygen. Historically, most of these reactions have utilized redox mediators, such as $CuCl_2$ or benzoquinone/macrocyclic-metal-complex mixtures, to promote aerobic oxidation of the reduced catalyst (Scheme 1).[1] It has been argued that redox mediators are needed because direct reactions between Pd^0 and O_2 are kinetically slow.[1b] Over the past decade, however, numerous catalytic reactions have been identified in which efficient catalytic turnover has been achieved with O_2 in the *absence* of redox mediators. These cocatalyst-free conditions have been applied to a wide variety of organic oxidation reactions, including alcohol oxidation and oxidative C−C, C−N, and C−O bond formation.[2]

One of the most difficult challenges in Pd-catalyzed aerobic oxidation reactions is the tendency of the catalyst to decompose into inactive metallic palladium via aggregation of Pd^0 (see Scheme 1).[3] The identification of catalysts that exhibit greater stability or undergo more efficient reoxidation by molecular oxygen would have a significant impact on this field. In order to facilitate the development of such catalysts, we have been investigating mechanisms of fundamental reactions between O_2 and Pd^0 species.[4–6] These studies highlight a stepwise sequence for the oxidation of Pd^0 by O_2 (**C** → **D** → **E** → **A**, Scheme 2).

Many Pd-mediated substrate oxidation reactions proceed via Pd^{II}-hydride intermediates (**B**, Scheme 2) that form during substrate oxidation (e.g., via β-hydride elimination). It has been widely assumed that the Pd^{II}-hydride species **B** undergoes reductive elimination of HX to yield Pd^0,[7] and regeneration of the Pd^{II} catalyst occurs via oxidation of Pd^0. This assumption

(1) (a) Henry, P. M. *Palladium-Catalyzed Oxidation of Hydrocarbons*; D. Reidel: Dordrecht, Holland, 1980. (b) Bäckvall, J.-E. *Acc. Chem. Res.* **1983**, *16*, 335–342.

(2) For reviews, see: (a) Stahl, S. S. *Angew. Chem., Int. Ed.* **2004**, *43*, 3400–3420. (b) Stahl, S. S. *Science* **2005**, *309*, 1824–1826. (c) Sigman, M. S.; Schultz, M. J. *J. Org. Biomol. Chem.* **2004**, *2*, 2551–2554. (d) Sigman, M. S.; Jensen, D. R. *Acc. Chem. Res.* **2006**, *39*, 221–229. (e) Stoltz, B. M. *Chem. Lett.* **2004**, *33*, 362–367. (f) Nishimura, T.; Uemura, S. *Synlett* **2004**, 201–216. (g) Sheldon, R. A.; Arends, I. W. C. E.; ten Brink, G.-J.; Dijksman, A. *Acc. Chem. Res.* **2002**, *35*, 774–781. (h) Toyota, M.; Ihara, M. *Synlett* **2002**, 1211–1222. (i) Muzart, J. *Tetrahedron* **2003**, *59*, 5789–5816.

(3) For discussion and analysis of Pd decomposition during catalytic turnover, see: Steinhoff, B. A.; Stahl, S. S. *J. Am. Chem. Soc.* **2006**, *128*, 4348–4355.

(4) Direct investigation of Pd reoxidation by O_2 under catalytic conditions has not been possible in any of the reactions reported to date. In every reaction studied thus far, the catalyst resting state consists of Pd^{II}, and the turnover-limiting step is associated with oxidation of the organic substrate. For leading references to mechanistic studies of reactions under catalytic conditions, see: (a) Mueller, J. A.; Goller, C. P.; Sigman, M. S. *J. Am. Chem. Soc.* **2004**, *126*, 9724–9734. (b) Steinhoff, B. A.; Guzei, I. A.; Stahl, S. S. *J. Am. Chem. Soc.* **2004**, *126*, 11268–11278.

(5) For highlights and reviews addressing catalyst reoxidation by O_2, see: (a) Popp, B. V.; Stahl, S. S. In *Organometallic Oxidation Catalysis*; Meyer, F., Limberg, C., Eds.; Springer: New York, 2007; Vol. 22, pp 149–189. (b) Gligorich, K. M.; Sigman, M. S. *Angew. Chem., Int. Ed.* **2006**, *45*, 6612–6615. (c) Muzart, J. *Chem. Asian J.* **2006**, *1*, 508–515.

(6) (a) Stahl, S. S.; Thorman, J. L.; Nelson, R. C.; Kozee, M. A. *J. Am. Chem. Soc.* **2001**, *123*, 7188–7189. (b) Konnick, M. M.; Guzei, I. A.; Stahl, S. S. *J. Am. Chem. Soc.* **2004**, *126*, 10212–10213.

Scheme 1. Traditional Mechanism for Palladium-Catalyzed Aerobic Oxidation Reactions

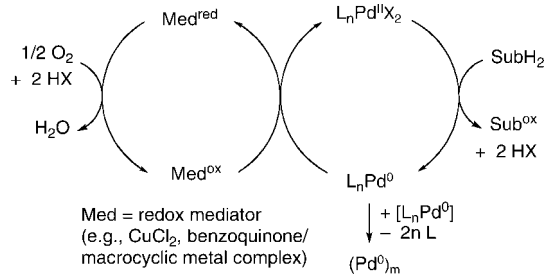

Scheme 2. Catalytic Cycle for Palladium-Catalyzed Aerobic Oxidation Reactions Highlighting Alternate Pathways for Catalyst Reoxidation by Molecular Oxygen

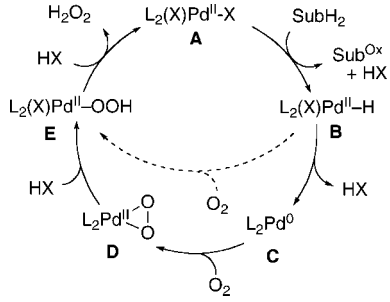

is evident in traditional Pd^{II}/Pd^0 catalytic cycles, such as that shown in Scheme 1. Several groups, however, have proposed that the Pd^{II}-hydride intermediate could react directly with O_2 to form the Pd^{II}-hydroperoxide intermediate **E** (Scheme 2, dashed arrow).[8] The prospect of direct Pd−H oxygenation is significant because, if this process occurs, unstable Pd^0 intermediates could be avoided during catalytic turnover (cf. Scheme 2). Our prior studies of the reaction of Pd^0 with O_2 cannot exclude this possibility, and, at the time we began our work, no precedents for reactions of O_2 with Pd^{II}-hydride species existed in the literature.

In order to investigate the reactivity of well-defined Pd^{II}-hydride complexes with molecular oxygen, we prepared complexes of the type *trans*-$(NHC)_2Pd^{II}(H)(O_2CR)$ (NHC = *N*-heterocyclic carbene; R = CH_3, Ph, *p*-$O_2NC_6H_4$), which closely mimic intermediates proposed to form in oxidation reactions mediated by NHC-coordinated Pd catalysts.[5a,9] We recently reported that $(IMes)_2Pd(H)(OBz)$, **1**, reacts with O_2 in benzene solution to produce the corresponding Pd-hydroperoxide product (eq 1).[10] Independently, Kemp and Goldberg reported that the PCP-pincer Pd-hydride complex **3** reacts with O_2 to yield the hydroperoxide **4**

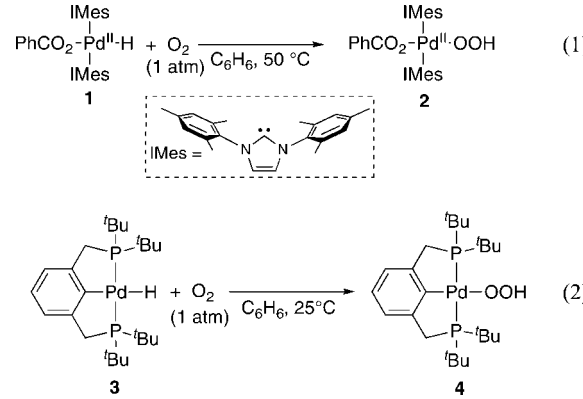

(eq 2).[11]

Previous studies of other transition-metal hydrides[12] suggest that a number of different mechanisms are possible for oxygenation of a Pd−H species (Scheme 3). A radical-chain autoxidation mechanism has been demonstrated in the reaction of O_2 with $Rh^{III}-H$,[12d,g,h] $Pt^{II}-H$,[12j] and $Pt^{IV}-H$[12k] species (cf. Scheme 3, Pathway 1). The oxygenation of certain $Rh^{III}-H$[12c,e,f] and $Ir^{III}-H$[12e,i] complexes has been proposed to be initiated by reductive elimination of HX, although little evidence for this pathway was provided (cf. Scheme 3, Pathway 2). A coordination−insertion mechanism has been suggested for oxygenation of a tris(pyrazolylborate)-coordinated $Co^{II}-H$ (cf. Scheme 3, Pathways 3 and 4).[12m]

Another mechanism for Pd−H oxygenation was proposed recently by Goddard and co-workers, who utilized DFT calculations to investigate the reaction of O_2 with the Pd−H complex [(−)-sparteine]Pd(H)Cl, **5**.[13] Their calculations support a pathway involving hydrogen-atom abstraction (HAA) by molecular oxygen, followed by inner-sphere rearrangement of a $Pd^{I}\cdots$HOO adduct to yield a Pd^{II}-hydroperoxide product (Scheme 4; cf. Scheme 3, Pathway 5). Experimental[11a] and computational[11b,14] studies of the oxygenation of (PCP)Pd−H complex **3** (eq 2) indicate that this reaction proceeds by an HAA mechanism.

(7) For studies of HX reductive elimination from Pd-hydride complexes, see: (a) Amatore, C.; Jutand, A.; Meyer, G.; Carelli, I.; Chiarotto, I. *Eur. J. Inorg. Chem.* **2000**, 1855–1859. (b) Hills, I. D.; Fu, G. C. *J. Am. Chem. Soc.* **2004**, *126*, 13178–13179.

(8) See, for example: (a) Muzart, J.; Pete, J. P. *J. Mol. Catal.* **1982**, *15*, 373–376. (b) Takehira, K.; Hayakawa, T.; Orita, H.; Shimizu, M. *J. Mol. Catal.* **1989**, *53*, 15–21. (c) Hosokawa, T.; Murahashi, S.-I. *Acc. Chem. Res.* **1990**, *23*, 49–54. (d) Hosokawa, T.; Nakahira, T.; Takano, M.; Murahashi, S.-I. *J. Mol. Catal.* **1992**, *74*, 489–498. (e) Nishimura, T.; Onoue, T.; Ohe, K.; Uemura, S. *J. Org. Chem.* **1999**, *64*, 6750–6755. (f) Nishimura, T.; Kakiuchi, N.; Onoue, T.; Ohe, K.; Uemura, S. *J. Chem. Soc., Perkin Trans. 1* **2000**, 1915–1918.

(9) (a) Jensen, D. R.; Schultz, M. J.; Mueller, J. A.; Sigman, M. S. *Angew. Chem., Int. Ed.* **2003**, *42*, 3810–3813. (b) Mueller, J. A.; Goller, C. P.; Sigman, M. S. *J. Am. Chem. Soc.* **2004**, *126*, 9724–9734. (c) Schultz, M. J.; Hamilton, S. S.; Jensen, D. R.; Sigman, M. S. *J. Org. Chem.* **2005**, *70*, 3343–3352. (d) Muñiz, K. *Adv. Synth. Catal.* **2004**, *346*, 1425–1428. (e) Rogers, M. M.; Wendlandt, J. E.; Guzei, I. A.; Stahl, S. S. *Org. Lett.* **2006**, *8*, 2257–2260.

(10) Konnick, M. M.; Gandhi, B. A.; Guzei, I. A.; Stahl, S. S. *Angew. Chem., Int. Ed.* **2006**, *45*, 2904–2907.

(11) (a) Denney, M. C.; Smythe, N. A.; Cetto, K. L.; Kemp, R. A.; Goldberg, K. I. *J. Am. Chem. Soc.* **2006**, *128*, 2508–2509. (b) Keith, J. M.; Muller, R. P.; Kemp, R. A.; Goldberg, K. I.; Goddard, W. A., III; Oxgaard, J. *Inorg. Chem.* **2006**, *45*, 9631–9633.

(12) Formation of metal-hydroperoxides via oxygenation of other transition-metal hydrides has been reported. Rhodium: (a) Roberts, H. L.; Symes, W. R. *J. Chem. Soc. A* **1968**, 1450–1453. (b) Johnston, L. E.; Page, J. A. *Can. J. Chem.* **1969**, *47*, 4241–4246. (c) Gillard, R. D.; Heaton, B. T.; Vaughan, D. H. *J. Chem. Soc. A* **1970**, 3126–3130. (d) Endicott, J. F.; Wong, C.-L.; Inoue, T.; Natarajan, P. *Inorg. Chem.* **1979**, *18*, 450–454. (e) Atlay, M. T.; Preece, M.; Strukul, G.; James, B. R. *Can. J. Chem.* **1983**, *61*, 1332–1338. (f) Gamage, S. N.; James, B. R. *Chem. Commun.* **1989**, 1624–1626. (g) Bakac, A. *J. Am. Chem. Soc.* **1997**, *119*, 10726–10731. (h) Bakac, A. *J. Photochem. Photobiol., A* **2000**, *132*, 87–89. Iridium: (i) Atlay, M. T.; Preece, M.; Strukul, G.; James, B. R. *Chem. Commun.* **1982**, 406–407. Platinum: (j) Wenzel, T. T. *Stud. Surf. Sci. Catal.* **1991**, *66*, 545–554. (k) Wick, D. D.; Goldberg, K. I. *J. Am. Chem. Soc.* **1999**, *121*, 11900–11901. Cobalt: (l) Bayston, J. H.; Winfield, M. E. *J. Catal.* **1964**, *3*, 123–128. (m) Thyagarajan, S.; Incarvito, C. D.; Rheingold, A. L.; Theopold, K. H. *Chem. Commun.* **2001**, 2198–2199.

(13) Keith, J. M.; Nielsen, R. J.; Oxgaard, J.; Goddard, W. A., III *J. Am. Chem. Soc.* **2005**, *127*, 13172–13179.

(14) Chowdhury, S.; Rivalta, I.; Russo, N.; Sicilia, E. *Chem. Phys. Lett.* **2007**, *443*, 183–189.

Scheme 3. Possible Mechanisms for the Reaction of O_2 with a Pd^{II}-Hydride To Produce a Pd^{II}-Hydroperoxide

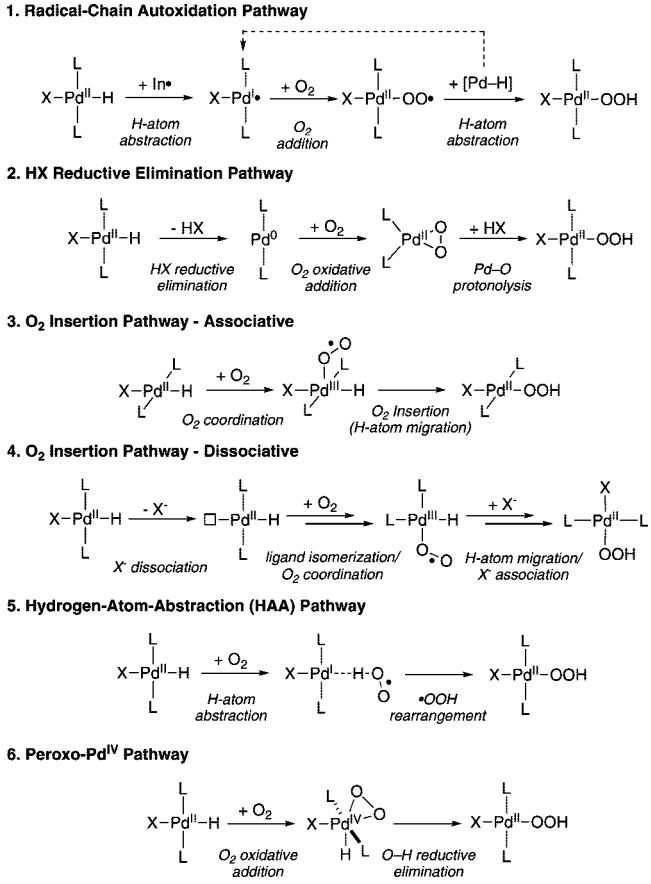

Scheme 4. Hydrogen-Atom-Abstraction (HAA) Pathway for Oxygenation of [(−)-Sparteine]Pd^{II}(H)Cl

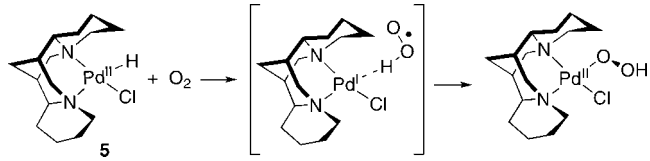

Diagnostic experimental data include determination of a bimolecular rate law (rate = k[Pd−H][O_2]), measurement of a large deuterium kinetic isotope effect ($k_{Pd-H}/k_{Pd-D} = 5.8$), and a lack of influence of radical traps and initiators on the rate.[11a]

A final mechanism to be considered consists of oxidative addition of O_2 to the Pd^{II} center to yield an η^2-peroxo-Pd^{IV} intermediate (Scheme 3, Pathway 6). Subsequent reductive elimination of an O−H bond would yield the hydroperoxide product. Examples of oxidative addition of O_2 to isoelectronic Ir^{I} and Rh^{I} species, such as Vaska's complex, are well known,[15] and accessing the Pd^{IV} oxidation state could be facilitated by the presence of strongly donating ligands (two NHC's and a hydride).

These mechanistic considerations highlight the numerous possible pathways for the oxygenation of Pd^{II}-hydride complexes. In a recent DFT computational study, we modeled the oxygenation of **1** (eq 1) and obtained evidence that the HAA pathway (Scheme 3, Pathway 5) exhibits the lowest barrier among the different mechanisms.[16] The calculated free-energy barrier for the HX-reductive-elimination pathway, however, was only slightly higher (4.8 kcal/mol). In the present study, we present an experimental mechanistic investigation of the oxygenation of $(IMes)_2Pd(H)(OBz)$, **1**, in benzene. The data support a mechanism for the reaction of O_2 with **1** that is initiated by reductive elimination of benzoic acid, and they are inconsistent with an HAA pathway. These observations align with the traditionally proposed Pd^{II}/Pd^0 cycle for Pd-catalyzed aerobic oxidation reactions. Analysis of our results and those reported previously by others suggests that most (if not all) of the known Pd-catalyzed aerobic oxidation reactions proceed via a Pd^{II}/Pd^0 catalytic cycle rather than a mechanism in which catalyst oxidation occurs via direct oxygenation of a Pd^{II}-hydride species.

Results

Characterization of the Reaction of $(IMes)_2Pd(H)(OBz)$, 1, with Molecular Oxygen in Benzene. The Pd^{II}-hydride complex $(IMes)_2Pd(H)(OBz)$, **1**, was prepared as described previously,[10] and its reaction with molecular oxygen in benzene-d_6 was evaluated by ^{1}H NMR spectroscopy. The resonances corresponding to the *ortho* and *para* methyl groups of the IMes ligands are intense, sharp singlets in the ^{1}H NMR spectrum at 1.99 ppm (24 protons) and 2.35 ppm (12 protons), respectively, and they are conveniently monitored during the reaction. When the reaction is performed in the presence of 1 atm O_2, oxygenation of **1** proceeds cleanly to the Pd^{II}-hydroperoxide **2** during the first half-life,[17] but, at later reaction times, numerous other peaks appear, corresponding to decomposition of the hydroperoxide species (Figure 1). On the basis of ^{1}H NMR spectroscopic and mass spectral (MALDI-TOF) data, we propose that the decomposition product arises from intramolecular oxygenation of a methyl group of the IMes ligand (eq 3; Figures S1–S3, Supporting Information).[18] Water, formed as a byproduct of this reaction, is evident in the ^{1}H NMR spectrum as a broad singlet at 0.52 ppm (Figure S1).

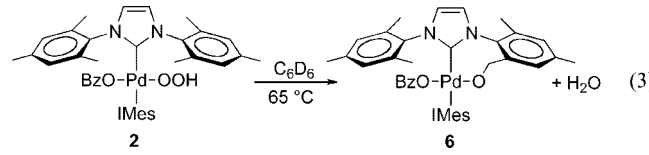

The nonexponential conversion of **1** into **2** (Figure 1B) complicated analysis of the kinetic data. By using initial-rates methods, however, it was possible to determine that the conversion of **1** into **2** in the presence of molecular oxygen exhibits a first-order dependence on **1** (Figure 2). Subsequently, it was determined that water, formed in the decomposition of **2** (eq 3), catalyzes the oxygenation of **1** and is the origin of the nonexponential kinetics. As shown in Figure 3, intentional addition of 10 equiv of water to the reaction mixture accelerates the oxygenation of **1**, and an exponential kinetic timecourse is

(15) (a) Vaska, L.; Chen, L. S.; Senoff, C. V. *Science* **1971**, *174*, 587–589. (b) Vaska, L. *Acc. Chem. Res.* **1976**, *9*, 175–183. (c) Valentine, J. S. *Chem. Rev.* **1973**, *73*, 235–245.

(16) Popp, B. V.; Stahl, S. S. *J. Am. Chem. Soc.* **2007**, *129*, 4410–4422.

(17) The Pd^{II}-OOH complex **2** has been prepared independently via protonolysis of $(IMes)_2Pd^{II}(\eta^2\text{-}O_2)$. See ref 6b and Supporting Information for details.

(18) See Supporting Information for further details. Analogous ligand oxidation has been observed previously for a cobalt-hydroperoxide complex (see ref 12m). In addition, ligand decomposition in Pd-catalyzed aerobic oxidation of alcohols has been proposed to proceed via the reaction of an (unobserved) hydroperoxide intermediate with a ligand benzylic methyl group: Conley, N. R.; Labios, L. A.; Pearson, D. M.; McCrory, C. C. L.; Waymouth, R. M *Organometallics* **2007**, *26*, 5447–5453.

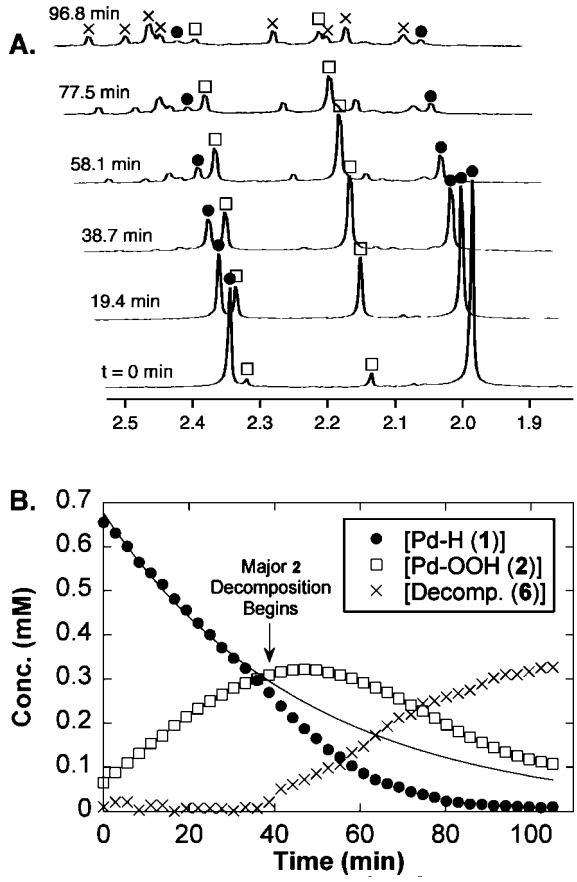

Figure 1. (A) Representative ^{1}H NMR spectra displaying the resonances associated with the *ortho* and *para* methyl groups of the IMes ligand during the reaction of Pd^{II}-hydride complex **1** with molecular oxygen. (B) Plot of the concentrations of $Pd^{II}-H$ **1**, $Pd^{II}-OOH$ **2**, and the decomposition product **6** during the course of the reaction. The solid line depicts the exponential decay of **1** that would be expected on the basis of the initial rate of the reaction. Reaction conditions: $[\mathbf{1}]_0 = 0.7$ mM, 1 atm O_2, 0.4 mL of C_6D_6, 65 °C.

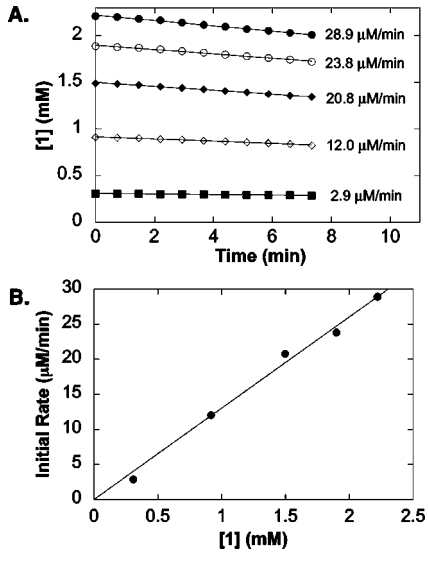

Figure 2. (A) Initial-rate kinetics data for the oxygenation of **1**. (B) Plot of the dependence of the initial rate on [**1**]. Reaction conditions: [**1**] = 0.31–2.2 mM, 3.7 atm O_2, 51 °C, C_6D_6.

observed under these pseudo-first-order conditions. The origin of this behavior will be discussed further below.

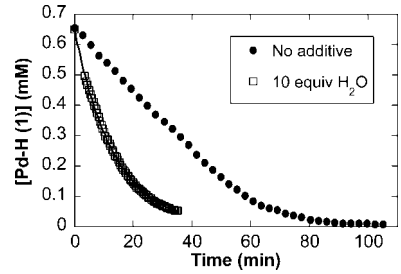

Figure 3. Comparison of the reaction timecourses for the oxygenation of **1** in the absence and in the presence of water. Reaction conditions: $[\mathbf{1}]_0 = 0.7$ mM, $[H_2O] = 0$, 7.0 mM, 1 atm O_2, 0.4 mL of C_6D_6, 65 °C.

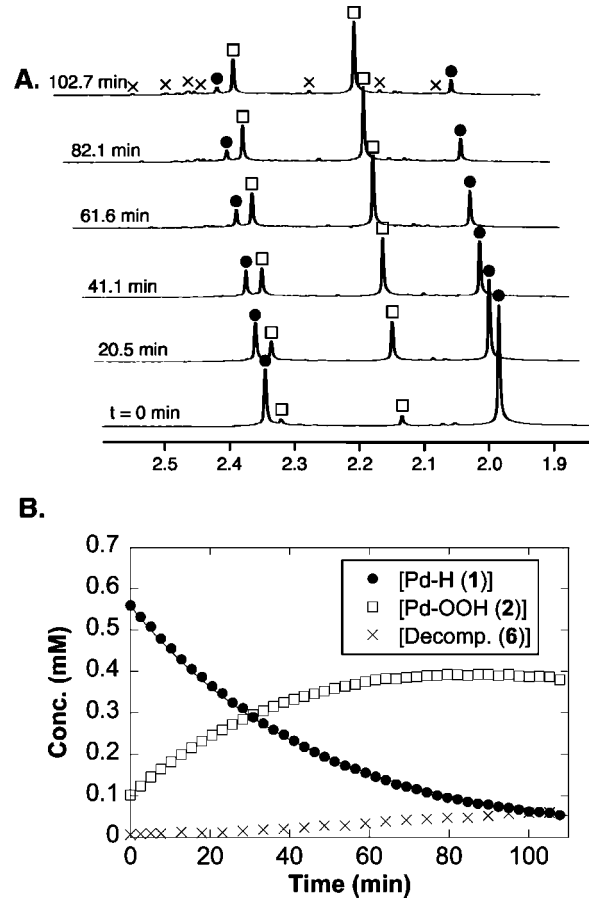

Figure 4. (A) Stacked plot of representative ^{1}H NMR spectra (displaying the region associated with the IMes methyl groups) for the aerobic oxygenation of $(IMes)_2Pd(H)(OBz)$, **1**, in benzene-d_6 in the presence of 1.75 equiv of NBu_4OBz. (B) Timecourse displaying the concentration of different species present during the reaction. Conditions: $[\mathbf{1}]_0 = 0.7$ mM, $[NBu_4OBz] = 1.22$ mM, 1 atm O_2, 0.4 mL of C_6D_6, 65 °C.

The effect of exogenous benzoate (NBu_4OBz) and benzoic acid on the oxygenation of **1** was investigated, and clean exponential conversion of **1** into **2** was observed in the presence of either additive. For example, in the presence of 1.75 equiv of NBu_4OBz, **1** reacts with O_2 to form **2**, with very little of the decomposition product detected until late in the reaction (Figure 4). Similar clean conversion of **1** into **2** is observed in the presence of 1.6 equiv of benzoic acid.[19] The reaction rate increases significantly in the presence of benzoic acid. The half-life of **1** is approximately 30 min in the absence of additives and in the presence of NBu_4OBz (Figures 1 and 4, respectively), but drops to less than 2 min in the presence of BzOH (Figure 5).

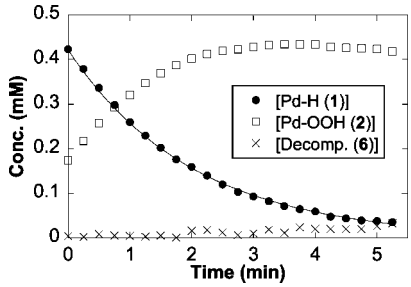

Figure 5. Timecourse of the aerobic oxygenation of $(IMes)_2Pd(H)(OBz)$, **1**, in the presence of added benzoic acid. Conditions: $[\mathbf{1}]_0 = 0.5$ mM, [BzOH] = 0.8 mM, 1 atm O_2, 0.4 mL of C_6D_6, 65 °C.

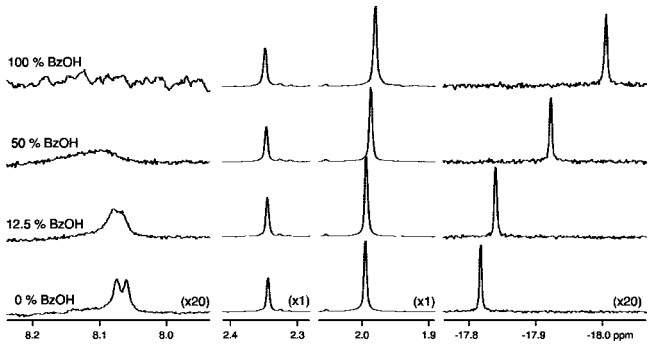

Figure 6. ^{1}H NMR spectra of **1** in the presence of different quantities of benzoic acid. Conditions: $[\mathbf{1}]_0 = 1.5$ mM, 1 atm O_2, 0.4 mL of C_6D_6, 39 °C.

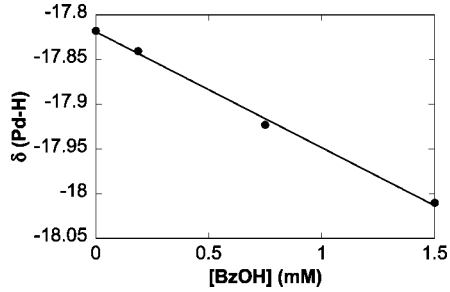

Figure 7. Plot of the Pd−*H* chemical shifts at different benzoic acid concentrations. Conditions: $[\mathbf{1}]_0 = 1.5$ mM, 1 atm O_2, 0.4 mL of C_6D_6, 39 °C.

Significant changes are evident in the ^{1}H NMR spectrum of **1** in benzene-d_6 when benzoic acid is present in the solution (Figure 6). For example, the *ortho* C−*H* resonances of the benzoate ligand at 8.08 ppm broaden significantly in the presence of 12.5 mol % benzoic acid and disappear into the baseline when a stoichiometric quantity of acid is present. The resonance of the hydride ligand at −17.82 ppm shifts upfield when benzoic acid is present, and the chemical shift exhibits a linear dependence on the BzOH concentration (Figure 7). Only minor effects of benzoic acid are detected on the carbene ligand resonances at 1.99 and 2.35 ppm.

The rate enhancements observed when the oxygenation of **1** is performed in the presence of water and benzoic acid appear to correlate with the protic character of these reagents. Confirmation of this hypothesis was obtained by adding to the reaction mixture catalytic quantities (0.25 equiv) of *p*-nitrophenol, a protic molecule that is unrelated to the reagents, products, or byproduct of the reaction. An exponential timecourse was observed, and the rate of the reaction was even faster than that observed in the presence of an identical quantity of benzoic acid (Figure 8). The timecourse obtained in the presence of NBu_4OBz is shown for comparison.

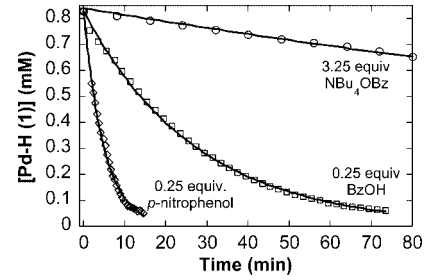

Figure 8. Exponential timecourses observed for the oxygenation of **1** in the presence of different additives. The reaction rate is significantly higher in the presence of protic additives BzOH and *p*-nitrophenol. Conditions: $[\mathbf{1}]_0 = 0.8$ mM, $[NBu_4OBz] = 2.6$ mM, [*p*-nitrophenol] = 0.2 mM, [BzOH] = 0.2 mM, 1 atm O_2, 0.4 mL of C_6D_6, 50 °C.

Kinetic Studies of the Reaction of $(IMes)_2Pd(H)(OBz)$, 1, with Molecular Oxygen in Benzene. The qualitative results presented above indicate that the oxygenation of **1** is well behaved kinetically when the reaction is performed in the presence of benzoate or benzoic acid, and they provide the basis for more thorough kinetic investigation of the oxygenation reaction. Rates of the oxygenation of **1** in the presence of different BzOH and NBu_4OBz concentrations were monitored by ^{1}H NMR spectroscopy. The disappearance of **1** fits cleanly to an exponential function under most conditions.[20] The reaction rate increases linearly with respect to the benzoic acid concentration (Figure 9A), whereas it is unaffected by changes to the benzoate concentration (Figure 9B). The rates measured in the presence of benzoate (Figure 9B) correspond to the value shown at the *y*-intercept in the [BzOH]-dependence plot in Figure 9A. Because exogenous benzoate enables the observation of clean exponential kinetics (cf. Figures 1B vs 4B), but has no influence the reaction rate, subsequent kinetic experiments were performed with NBu_4OBz (≥5 equiv) present in the reaction mixture.

Analysis of the effect of oxygen pressure on the oxygenation of **1** revealed that the rate does not depend on the oxygen pressure (0.32–3.3 atm, Figure 10). Clean exponential decay of **1** was observed even when only 2.9 equiv of dissolved O_2 relative to **1** was present in solution (Figure S4).[21] A deuterium kinetic isotope effect (KIE) was determined by preparing the Pd^{II}-deuteride, **1**-d_1, and comparing its rate of oxygenation with that of **1** (Figure 11). A small KIE, $k_H/k_D = 1.3(1)$, was detected.

(19) In our preliminary communication of the reaction between **1** and O_2 (ref 10), we reported clean, first-order kinetics for the oxygenation of **1** in the absence of additives. In subsequent studies, however, we determined that our original Pd-hydride samples contained trace amounts of BzOH that slightly increase the rate of the oxygenation reaction and result in clean, exponential kinetics. The BzOH originates from the synthesis of **1** and is not readily detected by NMR spectroscopy because it equilibrates with the BzO^- ligand coordinated to Pd (see Discussion later in this paper). In order to avoid this complication, subsequent syntheses of **1** were performed with a slight deficiency of BzOH relative to the Pd^0 precursor.

(20) Exponential disappearance of **1** is not observed when the reaction is performed in the absence of additives (NBu_4OBz and BzOH; see previous section for details) or at low benzoate concentrations; in these cases, initial rate data were used.

(21) Under the conditions of the NMR experiments, mass transfer of O_2 from the headspace into solution is slow. Therefore, only the dissolved O_2 concentration is relevant. In most of our experiments, we use 1 atm O_2, which corresponds to a dissolved O_2 concentration of ~9 mM in benzene. For discussions of O_2 solubility and issues related to mass-transfer into solution, see: (a) Steinhoff, B. A.; Guzei, I. A.; Stahl, S. S *J. Am. Chem. Soc.* **2004**, *126*, 11268–11278. (b) Steinhoff, B. A.; Stahl, S. S. *J. Am. Chem. Soc.* **2006**, *128*, 4348–4355.

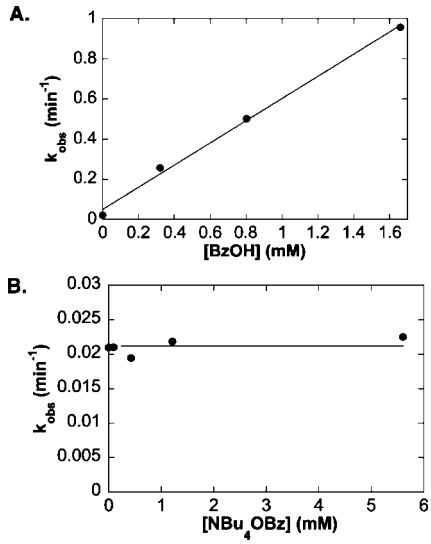

Figure 9. Effect of [BzOH] (A) and [NBu_4OBz] (B) on the observed rate constant for the oxygenation of **1** in benzene. Conditions: (A) $[\mathbf{1}]_0 = 0.5$ mM, [BzOH] = 0.0–1.66 mM, 1 atm O_2, 0.4 mL of C_6D_6, 65 °C; (B) $[\mathbf{1}]_0 = 0.7$ mM, [NBu_4OBz] = 0.0–5.6 mM, 1 atm O_2, 0.4 mL of C_6D_6, 65 °C.

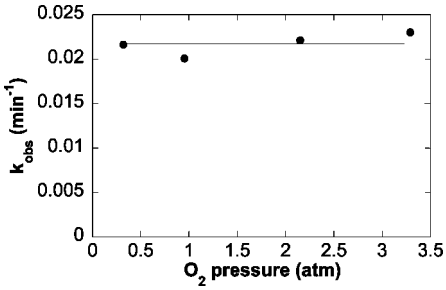

Figure 10. Effect of O_2 pressure on the observed rate constant for the oxygenation of **1** in benzene-d_6. Reaction conditions: $[\mathbf{1}]_0 = 1.0$ mM, $pO_2 = 0.32$–3.3 atm, [NBu_4OBz] = 13 mM, 0.4 mL of C_6D_6, 65 °C.

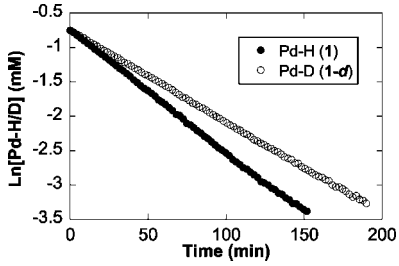

Figure 11. Reaction timecourses for the aerobic oxidation of **1** and **1**-d_1 in benzene-d_6. Reaction conditions: $[\mathbf{1}]_0$ and $[\mathbf{1}\text{-}d_1]_0 = 0.5$ mM, 1 atm O_2, [NBu_4OBz] = 8.1 mM, 0.4 mL of C_6D_6, 65 °C.

Measurement of the oxygenation of **1** at different temperatures enabled the determination of activation parameters by using an Eyring analysis (Figure 12): $\Delta H^{\ddagger} = 25.0(1)$ kcal/mol and $\Delta S^{\ddagger} = -0.8(4)$ eu.

In order to probe the possibility of a radical-chain autoxidation mechanism, we evaluated the reaction of **1** with O_2 in the presence of the radical initiator 2,2′-azobisisobutyronitrile (AIBN) and the radical inhibitor 2,6-di-*tert*-butyl-4-methylphenol (BHT). The oxygenation of **1** is essentially unaffected by the presence of either additive (Table 1). In fact, the rate

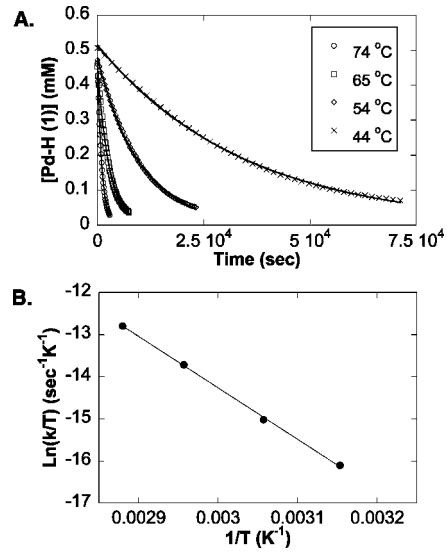

Figure 12. Kinetic timecourses reflecting the oxygenation of **1** in benzene-d_6 at different temperatures (A) and the corresponding Eyring plot (B). The activation parameters ($\Delta H^{\ddagger} = 25.0(1)$ kcal/mol and $\Delta S^{\ddagger} = -0.8(4)$ eu) were obtained by performing a global, nonlinear least-squares fit of the kinetic traces in panel A to the Eyring equation. Reaction conditions: $[\mathbf{1}]_0 = 0.5$ mM, 1 atm O_2, [NBu_4OBz] = 5.5 mM, 0.4 mL of C_6D_6, 44.0–74.1 °C.

Table 1. Effect of Radical Probes on the Aerobic Oxidation of $(IMes)_2Pd(H)(OBz)$, **1**, in C_6D_6[a]

entry	additive	k_{obs} (10^{-3}/min^{-1})[b]
1	none	22.0
2	0.1 mM AIBN[c] (17%)	18.0
3	0.4 mM BHT[d] (67%)	23.9

[a] Reaction conditions: $[\mathbf{1}]_0 = 0.6$ mM, $pO_2 = 1.0$ atm, [NBu_4OBz] = 5.6 mM, 65 °C, 0.4 mM C_6D_6. [b] $\pm 2.0 \times 10^{-3}$ min^{-1}. [c] AIBN = 2,2′-azobisisobutyronitrile. [d] BHT = 2,6-di-*tert*-butyl-4-methylphenol.

decreases slightly in the presence of the initiator AIBN and *increases* slightly in the presence of the inhibitor BHT. The rate also remains the same if the reaction is performed in the dark or in the presence of ambient room light.[22]

Solvent-Polarity and Anionic-Ligand Effects on the Oxygenation of $(IMes)_2Pd(H)(OBz)$, 1. The reaction of **1** with O_2 was investigated in solvents of higher polarity than benzene (dielectric constant, $\epsilon = 2.3$). Dissolution of **1** in coordinating solvents, including acetonitrile and THF, results in benzoate dissociation and formation of the ionic, solvent-coordinated species $[(IMes)_2Pd(H)(solvent)]^+OBz^-$. In order to avoid this complication, we identified solvents that are more polar than benzene but do not alter the identity of the ground-state Pd-hydride species. Suitable solvents included chlorobenzene ($\epsilon = 4.1$) and dichloromethane ($\epsilon = 9.1$). The rate of the reaction between **1** and O_2 increases significantly as the polarity of the solvent increases (Figure 13). The reaction is complete within minutes at room temperature in dichloromethane, whereas virtually no reaction is observed at this temperature in benzene.

(22) The mechanism of decomposition of the Pd-hydroperoxide species **2** (eq 3) has not been fully elucidated. The same decomposition product is observed if a radical inhibitor (BHT) is present in the reaction mixture; however, the decomposition rate is accelerated by the presence of ambient room light and AIBN. The decomposition of **2** yields a more-complicated product mixture when the reaction proceeds in the absence of O_2 or when the reaction is initiated by AIBN (in the presence of O_2). These empirical observations suggest that both radical and non-radical pathways might be involved.

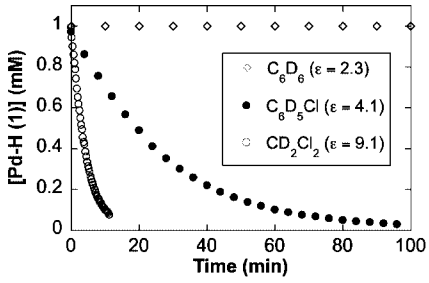

Figure 13. Effect of solvent on the rate for the oxygenation of **1** in benzene-d_6. Solvent dielectic constants are shown in parentheses next to the respective solvents. Reaction conditions: $[\mathbf{1}]_0 = 1.0$ mM, $pO_2 = 1.0$ atm, 0.4 mL of solvent, 25 °C.

In order to assess electronic effects associated with the carboxylate ligand, we prepared and investigated the oxygenation of two other Pd-hydride derivatives: *trans*-$(IMes)_2Pd^{II}(H)(O_2CAr)$ (Ar = *p*-$CH_3C_6H_4$, $\mathbf{1^{CH3}}$; *p*-$O_2NC_6H_4$, $\mathbf{1^{NO2}}$). The chemical shifts of Pd−H resonances in the ^{1}H NMR spectra of these compounds exhibit characteristic upfield and downfield shifts, respectively, relative to the parent benzoate derivative: δ −17.79 ($\mathbf{1^{CH3}}$), −17.82 (**1**), and −18.02 ($\mathbf{1^{NO2}}$). The oxygenation rate is enhanced by presence of more-electron-deficient carboxylate ligands: $k = 3.0 \times 10^{-4}$ ($\mathbf{1^{CH3}}$), 3.7×10^{-4} (**1**), and 22×10^{-4} s^{-1} ($\mathbf{1^{NO2}}$).

Discussion

Analysis of Possible Mechanisms for the Oxygenation of 1. Six different mechanisms were postulated for the reaction of $(IMes)_2Pd(H)OBz$, **1**, with O_2 (Scheme 3), and the results described above provide important constraints to distinguish among these possibilities. To summarize the kinetic data, the rate of the reaction of **1** with molecular oxygen exhibits a first-order dependence on [**1**] and a zero-order dependence on [O_2], [BzO^-], and radical probes. Benzoic acid can serve as a catalyst for the reaction, and, in its presence, the rate exhibits a first-order dependence on [BzOH]. These data are consistent with a relatively simple two-term rate law (eq 4). The first term corresponds to oxygenation of **1** in the absence of benzoic acid ($k_1 = 3.7 \times 10^{-4}$ s^{-1}), and the second term corresponds to the BzOH-catalyzed oxygenation reaction ($k_2 = 9.2$ M^{-1} s^{-1}). The reaction also exhibits a small deuterium isotope effect (KIE = 1.3).

$$\text{rate} = k_1[\mathbf{1}] + k_2[\mathbf{1}][\text{BzOH}] \quad (4)$$

The lack of a rate dependence on oxygen pressure excludes several proposed mechanisms from consideration, including associative O_2 insertion (Scheme 3, Mechanism 3), hydrogen-atom abstraction (Mechanism 5), and the peroxo-Pd^{IV} pathway (Mechanism 6). Each of these pathways is initiated by a bimolecular reaction of the Pd-hydride complex with O_2 and, therefore, should exhibit a first-order dependence on the O_2 concentration.[23] The near-zero entropy of activation ($\Delta S^{\ddagger} = -0.8(4)$ eu) provides additional evidence against a bimolecular rate-limiting step, and the small deuterium kinetic isotope effect is inconsistent with rate-limiting hydrogen-atom abstraction.[11]

(23) The prediction that these pathways will exhibit a first-order dependence on O_2 is based on the expectation that reaction of the Pd-hydride complex with O_2 will be the rate-determining step. The ^{1}H NMR spectrum of **1** is identical in the presence and in the absence of O_2, arguing against a ground-state interaction between O_2 and the Pd-hydride complex.

These results are distinctly different from the data for the oxygenation of (PCP)Pd−H complex **3** (see eq 2 and Introduction), which represents the only other Pd-hydride species whose reaction with O_2 has been studied experimentally.

Radical-chain autoxidation reactions can exhibit a zero-order dependence on the oxygen pressure; however, the lack of influence of radical probes and light on the reaction of **1** with O_2 argues against a radical-chain pathway (Scheme 3, Mechanism 1). Previously characterized metal-hydride oxygenation reactions that proceed by a radical-chain mechanism are very sensitive to the presence of radical probes (initiators, inhibitors) and/or light.[12dghjk] Although the operation of a radical-chain mechanism cannot be rigorously excluded by the lack of positive evidence, the observations provide strong justification for considering other possible mechanisms.

The two remaining mechanistic pathways include the HX-reductive-elimination and dissociative-O_2-insertion pathways (Mechanisms 2 and 4, respectively). Both of these mechanisms can account for the kinetic data if the initial steps of these mechanisms, reductive elimination of benzoic acid or dissociation of benzoate from **1**, constitute the *rate-limiting step* of the reaction (Scheme 5). Reductive elimination of benzoic acid from **1** to form $(IMes)Pd^0$, **9**, could occur by a concerted pathway, for example, via the five-membered, cyclic transition state **7** (Scheme 5, Pathway A), or by a stepwise mechanism, initiated by rate-limiting dissociation of benzoate from **1** to form the cationic Pd-hydride species **10** (Scheme 5, Pathway B). The dissociative-O_2-insertion pathway (Scheme 5, Pathway C) is also initiated by dissociation of benzoate from **1**.

The reaction rate for each of the three mechanisms shown in Scheme 5 is dictated by the rate of *formation* of **9** or **10**. Therefore, the overall reaction rate will be *independent of the [O_2]*, as observed experimentally. No rate dependence on [BzO^-] (as NBu_4OBz; Figure 9B) is expected with these mechanisms because concerted reductive elimination of benzoic acid should not be affected by exogenous benzoate and rate-limiting benzoate dissociation will not be subject to a common-ion effect. The solvent-polarity and carboxylate-electronic effects can be rationalized by these mechanisms. Transition states **7** and **8** would be expected to exhibit enhanced ionic character relative to the initial Pd^{II}-hydride structure **1**. Therefore, solvents with higher polarity and/or carboxylates with electron-withdrawing groups will stabilize the transition state and enhance the reaction rate. The small, normal KIE observed in the oxygenation of **1** ($k_H/k_D = 1.3$; Figure 11) may support the presence of a weak O···H interaction in the transition state as proposed for the concerted HX-reductive-elimination mechanism.[24]

The mechanisms in Scheme 5 provide a framework for understanding the catalytic role of benzoic acid and other protic additives, such as water (Figure 3) and *p*-nitrophenol (Figure 8). The ^{1}H NMR spectroscopic studies reveal that benzoic acid interacts with the Pd^{II}-hydride complex **1** (Figures 6 and 7), and the data are consistent with formation of a hydrogen-bonded adduct between benzoic acid and the carbonyl group of the coordinated benzoate ligand (**1·BzOH**, eq 5). This hydrogen-bonding interaction will enhance the oxygenation rate if it stabilizes the rate-limiting transition state (e.g., **7·BzOH** for concerted reductive elimination of BzOH or **8·BzOH** for benzoate dissociation) to a greater extent than it stabilizes the ground state (**1·BzOH**). This hypothesis seems reasonable because charge separation in benzene will be highly disfavored, and association of benzoic acid should stabilize the buildup of anionic charge on the benzoate ligand in transition states **7** and

Scheme 5. Possible Pathways for the Oxygenation of $(IMes)_2Pd(H)(OBz)$, **1**, in the Absence of Exogenous Benzoic Acid

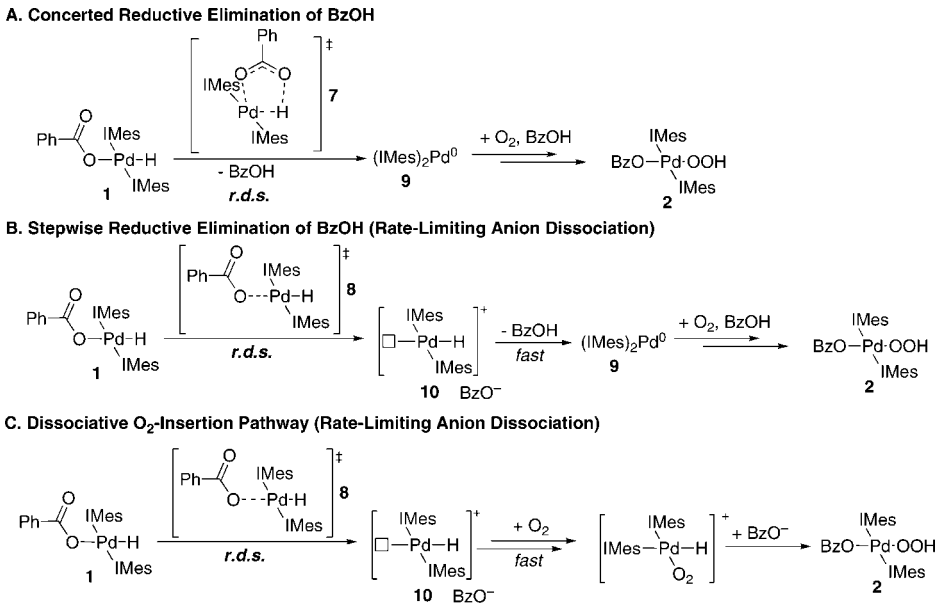

8. Moreover, structure **7·BzOH** should be more stable than transition state **7** because it exhibits much less structural distortion from the preferred square-planar geometry.

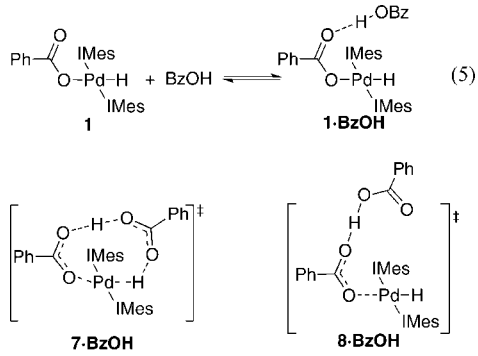

Comparison of Experimental and Computational Studies. The experimental data exclude a number of the original mechanistic proposals (Scheme 3), but they are limited in their ability to distinguish between the HX-reductive-elimination and dissociative-O_2-insertion pathways (Scheme 5). The findings of our recent computational study, however, strongly disfavor the O_2-insertion pathway. Density-functional theoretical methods were used to investigate the oxygenation of a model $(NHC)_2Pd(H)O_2CR$ complex, $(IMe)_2Pd(H)OAc$, **11**. The results reveal that two different mechanisms, H-atom abstraction and HX reductive elimination, are nearly isoenergetic and exhibit significantly lower barriers than other mechanisms (Figure 14). The O_2-insertion pathway is the least favorable among the pathways considered. The calculated free energy of the *intermediate* for O_2 insertion is nearly 30 kcal/mol higher than the highest *transition-state* energy in the HX-reductive-elimination pathway. The high energy of the O_2-insertion intermediate appears to have two origins: (1) the energetic cost of ion separation in a nonpolar solvent and (2) the weak affinity of O_2 for the cationic $[(IMe)_2Pd(H)]^+$ species. The O_2 fragment in the $[(IMe)_2Pd(H)O_2]^+OAc^-$ intermediate exhibits a calculated O−O bond length of 1.22 Å, only slightly longer than that in molecular oxygen (1.21 Å). This observation indicates that the three-coordinate Pd^{II} species $[(IMe)_2Pd(H)]^+$ is a poor reducing agent, incapable of reductive activation of O_2 to a generate a superoxide or peroxide species.

The calculated barriers for the two preferred pathways, H-atom abstraction and HX reductive elimination, compare favorably to the experimental free energy of activation calculated from the temperature-dependence data presented above, $\Delta G^{\ddagger} = 25.2(3)$ kcal/mol at 25.0 °C (Figure 12). Although the H-atom-abstraction pathway exhibits a lower calculated energy barrier than the HX-reductive-elimination pathway ($\Delta\Delta G^{\ddagger} = 4.8$ kcal/mol), computational analysis of other experimental observations supports the HX-reductive-elimination pathway. For example, computational studies of the role of carboxylic acid on the two oxygenation mechanisms revealed that the energy barrier for the HX-reductive-elimination pathway is *lower* in the presence of carboxylic acid, consistent with experimental observations (cf. Figure 9A), whereas the H-atom-abstraction mechanism exhibits a *higher* barrier in the presence of carboxylic acid.[16] Furthermore, the kinetic data presented above, in particular the zero-order dependence on $[O_2]$ and the small kinetic isotope effect, are inconsistent with the H-atom-abstraction mechanism. The HX-reductive-elimination pathway is the only mechanism supported by both experimental and computational data.

This comparative analysis highlights the synergy that exists between computational and experimental studies, but it also emphasizes the importance of experimental benchmarks for evaluating the computational results. Simple comparison of activation energies may not be sufficient. The calculated free-energy barriers in Figure 14 incorrectly favor the H-atom-abstraction mechanism. This error presumably reflects the intrinsic uncertainties associated with DFT calculations (e.g., the calculation of entropies, the comparison of calculated energies of charged versus uncharged species, and the use of implicit solvation models); however, it was possible to recognize

(24) A concerted reductive-elimination pathway has been identified by DFT calculations (see ref 16 and the discussion below), and the computations support a small isotope effect for this pathway. The calculated kinetic isotope effect for reductive elimination of acetic acid from a closely related model complex is 1.6. Popp, B. V.; Stahl, S. S., unpublished results.

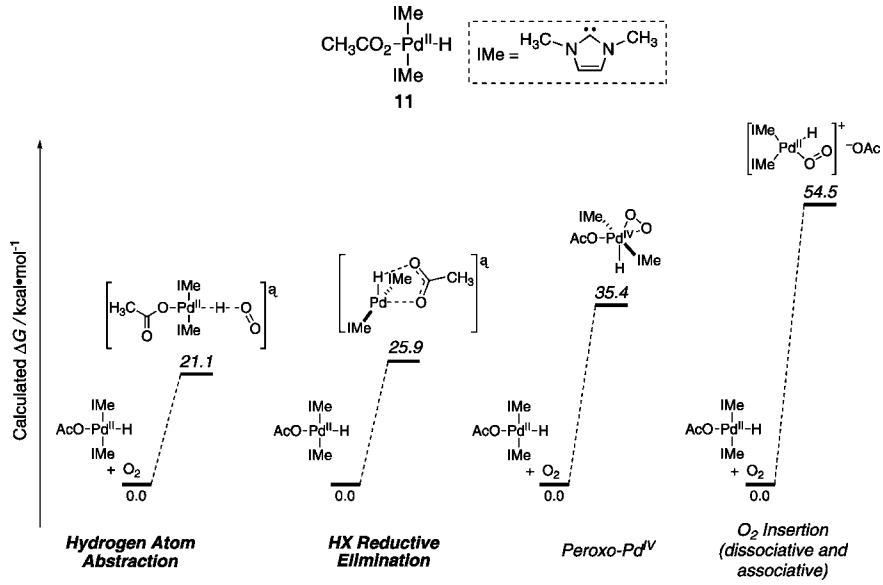

Figure 14. Calculated transition state and intermediate free energies for four different mechanisms for the oxygenation of $(IMe)_2Pd(H)OAc$, **11** (B3LYP; Stuttgart RSC 1997 ECP for Pd and 6-31+G(d) for C, N, O, H; toluene modeled as the solvent using a polarizable continuum model (IEF-PCM); 25 °C). See ref 16 for details.

this error by comparing other computational data with appropriate experimental results (e.g., the role of carboxylic acid on the reaction rate). These considerations are relevant to recent studies by Keith et al., who expanded their computational analysis of the oxygenation of [(−)-sparteine]Pd(H)Cl, **5** (cf. Scheme 4).[13,25] Upon calculating the energy barrier of the HX-reductive-elimination pathway, they conclude that this mechanism is not operative because the calculated free-energy barrier is 7.5 kcal/mol higher than that of the H-atom-abstraction pathway. Although this $\Delta\Delta G^{\ddagger}$ is 2.7 kcal/mol larger than the free energy difference we calculate for the oxygenation of **11** ($\Delta\Delta G^{\ddagger}$ = 4.8 kcal/mol), their conclusion has not yet been validated experimentally.

Conclusions

The experimental studies described here, together with the computational results reported previously,[16] provide compelling evidence that oxygenation of $(NHC)_2Pd(H)O_2CR$ complexes proceeds via a pathway initiated by rate-limiting reductive elimination of carboxylic acid. Rapid addition of O_2 to the resulting Pd^0 species, and subsequent reaction of the η^2-peroxo-Pd^{II} species with the carboxylic acid generated in the reductive-elimination step, yields the Pd^{II}-hydroperoxide product. This three-step process for conversion of a Pd^{II}-hydride into a Pd^{II}-hydroperoxide is preferred over a hydrogen-atom-abstraction pathway, direct O_2 insertion, and several other possible mechanisms. The results provide the first direct experimental evidence for the traditional Pd^{II}/Pd^0 redox cycle proposed for Pd-catalyzed aerobic oxidation reactions, and they differ significantly from the recent results of Kemp and Goldberg in their study of the oxygenation of the (PCP)Pd-hydride complex **3**,[11] which proceeds by a hydrogen-atom-abstraction mechanism.

The divergent mechanisms established for the oxygenation of $(IMes)_2Pd(H)OBz$ (**1**) and (PCP)Pd(H) (**3**) suggest that different catalyst reoxidation pathways might occur with different Pd catalysts in aerobic oxidation reactions, and further studies will be needed to elucidate the factors that promote the different reaction pathways. The (PCP)Pd(H) complex does not have a readily accessible reductive-elimination pathway available; the aryl ligand *trans* to the hydride in **3** is a strong σ-donor that will weaken the Pd−H bond and facilitate H-atom abstraction.[26] In contrast, complex **1** features a weakly donating benzoate ligand *trans* to the hydride that will disfavor Pd−H bond homolysis and is capable of undergoing reductive elimination of benzoic acid. Carboxylic acid reductive elimination should be even more facile from complexes that can achieve a *cis* relationship between the hydride and carboxylate ligands. Common catalyst systems employed in aerobic oxidation reactions, such as $Pd(OAc)_2$/pyridine, $Pd(OAc)_2$/DMSO, and monocarbene ligated Pd complexes, feature labile, neutral-donor ligands that should be capable of achieving such a geometry. Therefore, we postulate that the common Pd catalysts discovered to date for aerobic oxidation reactions, with the possible exception of catalysts bearing chelating nitrogen ligands,[25] proceed via Pd^{II}/Pd^0 catalytic cycles.

Experimental Section

General Considerations. All procedures, except for the oxygenation reactions, were carried out under an inert atmosphere of nitrogen in an inert atmosphere glovebox or by using standard Schlenk techniques. Benzoic acid, 1,3,5-trimethoxybenzene, AIBN, BHT, and oxygen gas were used without purification. NBu_4OBz was recrystallized prior to use from pentane/ether. Benzoic acid-d_1 was prepared by dissolving benzoic acid in methanol-d_4 followed by evaporation of the methanol-d_4; this procedure was repeated six times. All solvents used were dried and deoxygenated prior to usage: diethyl ether, pentane, and toluene were passed through a column of activated alumina and Q4. C_6D_6 was degassed and dried by distillation from Na/benzophenone; CD_3CN was degassed and dried by distillation from CaH_2. Infrared spectra were obtained with a

(25) Keith, J. M.; Goddard, W. A., III; Oxgaard, J. *J. Am. Chem. Soc.* **2007**, *129*, 10361–10369.

(26) The role of the *trans*-effect of the ligand *trans* to the hydride was addressed in our recent computational study (ref 16), in which we compared H-atom abstraction from *trans*-$(IMe)_2Pd(H)OAc$ and *trans*-$(IMe)_2Pd(H)Me$. The free-energy barrier for H-atom abstraction by O_2 is lower by 6.4 kcal/mol when the hydride ligand is *trans* to a methyl group rather than a carboxylate ligand.

Brüker Tensor 25 spectrometer that was equipped with a single reflection MIRacle Horizontal ATR ZnSe crystal. NMR data were recorded using Varian Inova spectrometers (^{1}H: 500 or 600 MHz). Spectra recorded at elevated temperatures were calibrated with ethylene glycol. ^{1}H chemical shifts were referenced to residual protons in the deuterated solvent, benzene-d_6: 7.16 ppm. ^{13}C chemical shifts were referenced to the center line of the C_6D_6 triplet: 128.39 ppm.

General Procedure for Kinetic Studies of the Oxygenation of 1. A stock solution of internal standard (5.9 mM 1,3,5-trimethoxybenzne in 10 mL of C_6H_6) was prepared in a glovebox. Stock solutions of **1** and various additives were prepared by dissolving them in the C_6H_6 solution containing the internal standard, and the concentrations of these species were established by ^{1}H NMR spectroscopy. These solutions were added to a Wilmad J-Young NMR tube of known volume to achieve the desired concentrations when diluted to 0.400 mL. The NMR tube was connected to a gas manifold equipped with a volume-calibrated mercury manometer. The solution was degassed and filled with the desired pressure of O_2. Elevated pressures of O_2 were achieved by cooling the tube with liquid N_2. The tube was sealed and kept frozen in a dry ice/acetone bath until it was inserted into the preheated spectrometer probe. Multiple scans were taken for each data point, with the delay between acquisitions of $>5T_1$ ($T_1 \approx 1.2$ s under 1 atm O_2).

Data Fitting Procedures. Rate constants in benzene were determined from a nonlinear least-squares fit of an exponential function to the reaction timecourses using the Solver function within Microsoft Excel. Values for $[\mathbf{1}]_0$, k_1, and $[\mathbf{1}]_{infinity}$ were floated. Activation parameters in benzene were determined by performing a global, nonlinear-least-squares fit of the data (exponential timecourses obtained at four different temperatures) to the Eyring equation. The values of $[\mathbf{1}]_0$, $[\mathbf{1}]_{infinity}$, $\Delta H^{\ddagger}$, and $\Delta S^{\ddagger}$ were floated. Error analysis was carried out by applying the SOLVSTAT macro in Microsoft Excel to the data and solved parameters.[27]

Acknowledgment. We thank B. V. Popp and C. R. Landis for valuable discussions and the National Science Foundation for financial support of this work (CHE-0543585).

Supporting Information Available: Procedures for the synthesis and characterization of hydride **1** and hydroperoxide **2**, analysis of the decomposition product **6**, full ^{1}H NMR spectra obtained during the oxygenation of **1** in the presence and absence of NBu_4OBz, and exponential fit of the decay of **1** at low O_2 pressure. This material is available free of charge via the Internet at http://pubs.acs.org.

JA7112504

(27) Billo, E. J. *EXCEL for Chemists, a Comprehensive Guide*, 2nd ed.; John Wiley & Sons, Inc.: New York, 2001.